PCCP

PAPER

View Article Online
View Journal | View Issue

Published on 25 March 2014. Downloaded by Ruhr Universitat Bochum on 3/29/2023 1:12:20 PM.

Cite this: *Phys. Chem. Chem. Phys.*, 2014, **16**, 8441

Structure and properties of bimetallic titanium and vanadium oxide clusters

Benjamin Helmich,[ab] Marek Sierka,†[a] Jens Döbler[a] and Joachim Sauer*[a]

Received 20th February 2014,
Accepted 17th March 2014

DOI: 10.1039/c4cp00752b

www.rsc.org/pccp

By employing a genetic algorithm together with density functional theory (B3LYP), we investigate the most stable minimum structures of several bimetallic titanium and vanadium oxide clusters that contain four metal atoms. The following compositions are studied: $V_nTi_{n-4}O_{10}^-$ (n = 1–4), $(TiO_2)VO_n^-$ (n = 1–4), and $(TiO_2)VO_n^+$ (n = 1–3). Apart from $(TiO_2)_3VO^-$, vanadium oxo groups are always part of the most stable minimum structures when vanadium is present. Anti-ferromagnetic coupling lowers the energy substantially if spin centers are located at neighbored metal atoms rather than at distant oxygen radical sites. Vanadium-rich or oxygen-poor compositions prefer symmetric adamantane-like cage structures, some of which have already been proposed in a previous study. In contrast, vanadium-poor and oxygen-rich compositions show versatile structural motifs that cannot be intuitively derived from the symmetric cage motif. Particularly, for $Ti_4O_{10}^-$ there are several non-symmetric and distorted cages that have an up to 68 kJ mol^{-1} lower energy than the symmetric adamantane-like cage structure. Nevertheless, for the adamantane-like cage the simulated infra-red spectrum (within the harmonic approximation) agrees best with the experimental vibrational spectrum. The oxidative power of the $(TiO_2)_3VO_3^-$ and $(TiO_2)_3VO_2^+$ clusters as measured by the energy of removing 1/2 O_2 (297 and 227 kJ mol^{-1}, respectively) is less than that of the pure vanadium oxide clusters $(V_2O_5)VO_3^-$ and $(V_2O_5)VO_2^+$ (283 and 165 kJ mol^{-1}, respectively).

I. Introduction

Vanadium(V) oxide (V_2O_5) supported on other metal oxides such as TiO_2 is an important solid catalyst with applications in several industrial processes[1,2] like the oxidation of SO_2.[3] It is also used for selective oxidation of methanol to formaldehyde and propane to propene. This material has therefore been chosen for experimental and theoretical studies of the strong dependency of the catalytic activity on the supporting oxide.[2,4–6]

Experimental and computational investigations of catalytically active species on surfaces of solid catalysts are very challenging, because often the size and distribution of the active species are not known. From infra-red (IR) and Raman spectroscopic studies it has been concluded that, primarily, monomeric vanadyl species are formed when a highly active vanadia monolayer is dispersed on the anatase surface,[7,8] but it has also been shown that spectroscopic discrimination between monomeric and polymeric species is difficult.[9]

Therefore, besides thin film models that are studied by surface science techniques,[9] isolated gas-phase clusters are employed as models of the active sites. For example, surface science studies on vanadium oxide species on the $CeO_2(111)$ surface[10,11] and IR studies on $Ce_mV_nO_o^+$ mixed metal oxide clusters[12] yielded a consistent picture of the redox behavior in these mixed metal oxide systems. Although gas phase models cannot be directly applied to investigate the precise mechanisms and kinetics operating in heterogeneous catalysis, they provide a conceptual framework and an efficient means to obtain insight into the structural features of active sites, reactivity patterns, and the nature of crucial intermediates.[13] The composition, charge, oxidation state, and degree of coordination of the clusters can be controlled and eventually compared to the results of reactivity experiments on isolated clusters,[14] see ref. 15 and 16 for other mixed metal vanadium oxide clusters.

The present study aims at modeling possible reactive sites and intermediates that appear in redox reactions at monomeric vanadyl species on a TiO_2 surface. These species are modeled by bimetallic oxide clusters with different charges and are composed of a single vanadium atom, three titanium atoms and a varying number of oxygen atoms depending on the degree of reduction. We start from a cluster model $(TiO_2)_3VO_4^-$ of over-oxidized monomeric vanadyl species that is subsequently deoxygenized in three steps. All cluster compositions $(TiO_2)_3VO_{1-4}^{+/-}$ are subject of our investigation.

[a] *Humboldt-Universität zu Berlin, Institut für Chemie, Unter den Linden 6, D-10099 Berlin, Germany. E-mail: js@chemie.hu-berlin.de*

[b] *Lehrstuhl für Theoretische Chemie, Ruhr-Universität Bochum, D-44801 Bochum, Germany. E-mail: benjamin.helmich@rub.de*

† Current address: Otto-Schott-Institut für Materialforschung, Friedrich-Schiller-Universität Jena, Löbdergraben 32, D-07743 Jena, Germany. E-mail: marek.sierka@uni-jena.de

Published on 25 March 2014. Downloaded by Ruhr Universitat Bochum on 3/29/2023 1:12:20 PM.

The composition-dependent properties of bimetallic oxide clusters of vanadium and titanium $V_{4-n}Ti_nO_{10}^-$ with n = 1–4 were characterized before by infrared multi-photon dissociation (IRMPD) spectroscopy in combination with density functional theory (DFT).[17] The respective cluster structures were constructed by so-called isomorphous substitutions where each vanadium atom in the adamantane-like cage structure of $V_4O_{10}^-$ (ref. 18) is exchanged by a titanium atom. The simulated vibrational spectrum of $V_4O_{10}^-$ can fully explain the experimental IRMPD spectrum when the B3LYP[19–21] functional in conjunction with the TZVP basis set[22] is employed.[18] Moreover, Janssens *et al.* found that the titanium-doped clusters show a much higher reactivity than the pure vanadium oxide cluster for the SO_2 oxidation,[23] as is observed in industrial catalysts.

Since the previous studies on $V_{4-n}Ti_nO_{10}^-$ (n = 1–4) clusters a hybrid *ab initio* genetic algorithm (HAGA)[24] became available that has successfully been applied in joint experimental and theoretical studies of other metal oxide gas phase clusters.[25–28] One of the aims of the present study is to check if the proposed $V_{4-n}Ti_nO_{10}^-$ (n = 1–4) cage structures are indeed global minima on the potential energy surface. Therefore, structure optimizations are performed for all cluster compositions and different spin states employing the genetic algorithm.

II. Computational details

All DFT calculations with the B3LYP exchange–correlations functional[19–21] were performed using the TURBOMOLE program package[29,30] employing a split-valence basis set augmented with polarization functions (SVP).[31] To speed up the evaluation of the Coulomb term the multipole accelerated resolution of identity (MARI-J) method was employed.[32] Global structure optimizations were performed using the DoDo program package.[33] For cluster compositions with an even (uneven) number of electrons, we performed GA optimizations of the singlet and triplet (doublet and quartet) spin states. Broken symmetry configurations are obtained by checking for triplet instabilities[34] of the spin restricted SCF wavefunction. The most stable final structures were locally optimized using a triple-ζ basis set augmented with polarization functions[31,35] (def2-TZVP), which yields energies close to the basis set limit in our DFT calculations. Harmonic vibrational frequencies were calculated for the final structures employing analytical second derivatives.[36]

III. Results and discussion

A. Global minima of $V_{4-n}Ti_nO_{10}^-$ (n = 1–4)

Previously, the structures of the $V_{4-n}Ti_nO_{10}^-$ clusters (n = 1–4) were obtained by substitution of vanadium for titanium starting from the T_d-symmetric adamantane-like cage structure of $V_4O_{10}^-$ (see Fig. 1) and subsequent local structure optimization.[17] The $V_4O_{10}^-$ structure itself was found to explain its IRMPD spectrum very well.[18] These clusters preserve the initial adamantane-like cage structure of $V_4O_{10}^-$ with six bridging oxo groups. To compensate for the decreasing positive charge on the metal sites as n goes from 1 to 4, the negative charge must also decrease resulting in a change from terminal oxo groups to terminal oxyl radicals (see Table 1). It was proposed that these structures in a high-spin configuration are global minima and can explain the experimental IRMPD spectra. In $Ti_4O_{10}^-$ isomorphous substitution leads to three terminal oxyl radicals **4d** with three unpaired electrons raises doubts whether the previously proposed cage structure is a global minimum for $Ti_4O_{10}^-$.

Low-lying minimum structures for $V_{4-n}Ti_nO_{10}^-$ with n = 1–4 obtained with our global optimization procedure are presented

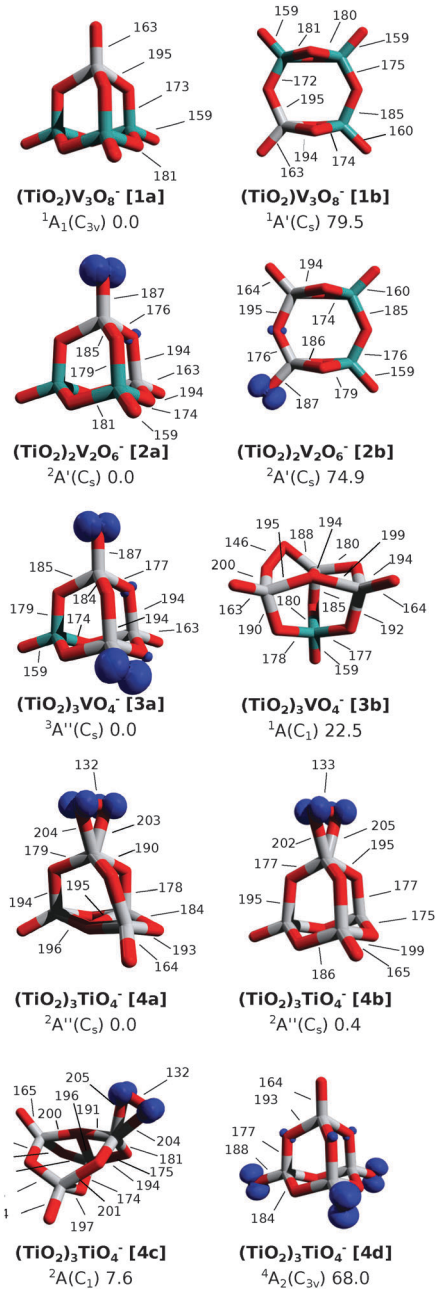


Fig. 1 B3LYP/TZVP optimized global minimum and selected local minimum structures of $V_{4-n}Ti_nO_{10}^-$-clusters with n = 1–4 along with their electronic state and symmetry point group. Energies relative to the global minimum in kJ mol^{-1}. Bond distances in pm. For open-shell systems iso-surfaces of the spin density are plotted (blue, iso-value 0.02).

 This journal is © the Owner Societies 2014

Published on 25 March 2014. Downloaded by Ruhr Universitat Bochum on 3/29/2023 1:12:20 PM.

Table 1 Charge of cationic q_M/e and anionic q_O/e species, the number of terminal oxo groups =O and terminal oxyl radicals $-O^{\bullet}$, and the spin state S for adamantane-like cages $V_{4-n}Ti_nO_{10}^-$ (n = 1–4). The number of bridging oxo groups is 6 for all the cages below

Cluster	q_M/e	q_O/e	=O	$-O^{\bullet}$	S
$V_3TiO_{10}^-$	+19	−20	4	0	s
$V_2Ti_2O_{10}^-$	+18	−19	3	1	d
$VTi_3O_{10}^-$	+17	−18	2	2	t
$Ti_4O_{10}^-$	+16	−17	1	3	q

in Fig. 1. The most stable structure for $V_3TiO_{10}^-$ is the singlet state adamantane-like cage **1a** with four terminal oxo groups, which is identical to the cage structure of ref. 17. As with $V_4O_{10}^-$,[37] the second most stable cluster **1b** of this composition features a ring structure and has a 79.5 kJ mol^{-1} higher energy than the global minimum. The triplet state global minimum is 202.5 kJ mol^{-1} higher in energy than the singlet state global minimum **1a**.

The global minimum structure of $V_2Ti_2O_{10}^-$ is an adamantane-like cage **2a** with a doublet ground state. The unpaired electron is located in the p-orbital of the terminal oxyl radical bonded to a titanium atom. Furthermore, **2a** has three terminal oxo groups. This structure was also obtained by isomorphous substitution in ref. 17. The second most stable cluster **2b** (+74.9 kJ mol^{-1}) has a ring structure with three terminal oxo groups and one oxyl radical bonded to a titanium atom. The most stable quartet state is 191.9 kJ mol^{-1} above the doublet state **2a**.

The most stable structure **3a** for $VTi_3O_{10}^-$ features an adamantane-like cage structure as predicted in ref. 17. Each of the two unpaired electrons which form a triplet ground state is located in a p-orbital of a terminal oxyl radical bonded to a titanium atom. Each of the two oxo groups is bonded to a vanadium atom. The second most stable structure **3b** has no unpaired electrons and features a distorted and non-symmetric cage structure. Instead of two terminal oxyl radicals, **3b** features a bridging peroxo unit between two titanium atoms. With 22.5 kJ mol^{-1} **3b** has a significantly smaller energy gap to the global minimum structure **3a** than **1b** and **2b**.

In the case of $Ti_4O_{10}^-$, there are several low-lying minima with a lower energy than the structure **4d** proposed by isomorphous substitution in ref. 17. The three most stable clusters **4a–c** share a titanium atom with a bond to a terminal superoxo unit, where a single unpaired electron is delocalized over the p-orbitals of two oxygen atoms. Each of the clusters **4a–c** has two further titanium atoms with a bond to a terminal oxo group and a three-fold coordinated titanium atom with a free binding site. The two most stable structures **4a–b** differ in energy by 0.4 kJ mol^{-1} only and feature a symmetric cage structure where the superoxo group lies inside the mirror plane. Their structures merely differ by a bridging oxo group that, in case of **4a**, is displaced towards the interior of the cage. The activation energy to convert **4a** into **4b** is 34.9 kJ mol^{-1}. Isomer **4d** has the lowest energy for three unpaired electrons in a quartet state, but features a 68 kJ mol^{-1} higher energy than the global minimum structure **4a** with a single unpaired electron in a doublet state. Each of the three unpaired electrons of **4d** is located in a p-orbital of a terminal oxyl radical bonded to a titanium atom.

In contrast to the adamantane-like cage structures with no (**1a**) or one (**2a**) unpaired electron, energy lowering for the cages **3a** and **4d** might also be achieved by means of anti-ferromagnetic coupling. But the broken-symmetry solutions with one spin-up and one spin-down for **3a** and two spin-up and one spin-down for **4d** yield energies that are slightly higher (0.1 and 0.2 kJ mol^{-1}) than their high-spin configuration counterparts. These spin centers in **3a**, **4d**, and in their broken-symmetry analogs are separated by approximately 600 pm and four Ti–O bonds so that exchange coupling through space or through bonds[38] does not play a substantial role here.

For the vanadium-rich compositions $V_3TiO_{10}^-$ and $V_2Ti_2O_{10}^-$, symmetric cages in a low-spin state are 70 kJ mol^{-1} significantly more stable than other clusters with different structural motifs and spin states. For $VTi_3O_{10}^-$ the stability of the adamantane-like cage **3a** is much less pronounced than for the vanadium-rich compositions, where the energetic difference to a distorted cage in a triplet state (**3b**) is only 22.5 kJ mol^{-1}. For $Ti_4O_{10}^-$ the symmetric cage in a quartet state with three terminal oxyl radicals has even a distinctively higher energy than the global minimum structure **4a**. Therefore, only the global minimum structures **1a**, **2a**, and **3a** coincide with the ones proposed by the isomorphous substitution scheme and feature an adamantane-like cage structure.

The energy separation of the most stable to the second most stable structure decreases with an increasing number of titanium atoms, from 79.5 kJ mol^{-1} for $V_3TiO_{10}^-$ to 0.4 kJ mol^{-1} for $Ti_4O_{10}^-$. By comparing the minimum structures of $V_{4-n}Ti_nO_{10}^-$ with n = 1–4, we can conclude that with an increasing number of titanium atoms terminal oxyl radicals become much less favorable, which results in global minimum structures that are less symmetric and tend to avoid unpaired electrons.

B. Vibrational spectra of $Ti_4O_{10}^-$

The GA optimization yields several low-lying minimum structures for $Ti_4O_{10}^-$. To investigate which of the structures is observed experimentally, we compare the calculated IR vibrational spectra with the experimental IRMPD spectrum of ref. 17. Fig. 2 shows the computed spectra of the three most stable minimum structures in the doublet state (**4a–c**) and the most stable minimum structure in the quartet state (**4d**) as well as the experimental IRMPD spectrum of $Ti_4O_{10}^-$ from 500 to 1100 cm^{-1}.

The experimental spectrum exhibits three characteristic ranges. An intense and sharp band at around 970 cm^{-1}, a very intense and broad band with possible shoulders between 780 and 880 cm^{-1} and a less intense and very broad band between 570 and 730 cm^{-1} which may contain several vibrational modes that cannot be resolved. The sharp band at around 1000 cm^{-1} is present in the simulated spectra of all structures **4a–d**. It can be assigned to symmetric and antisymmetric (only for **4a–c**) stretching modes of terminal oxo groups, which are common to all four structures. Furthermore, the four clusters exhibit several intense modes in the range of 750–900 cm^{-1} associated with bond stretching of bridging oxo groups within the adamantane cage. The frequencies of these modes strongly differ amongst the four clusters, which can be attributed to the respective cage structure. The modes of **4b** and **4d** are located in a rather small range of

Published on 25 March 2014. Downloaded by Ruhr Universitat Bochum on 3/29/2023 1:12:20 PM.

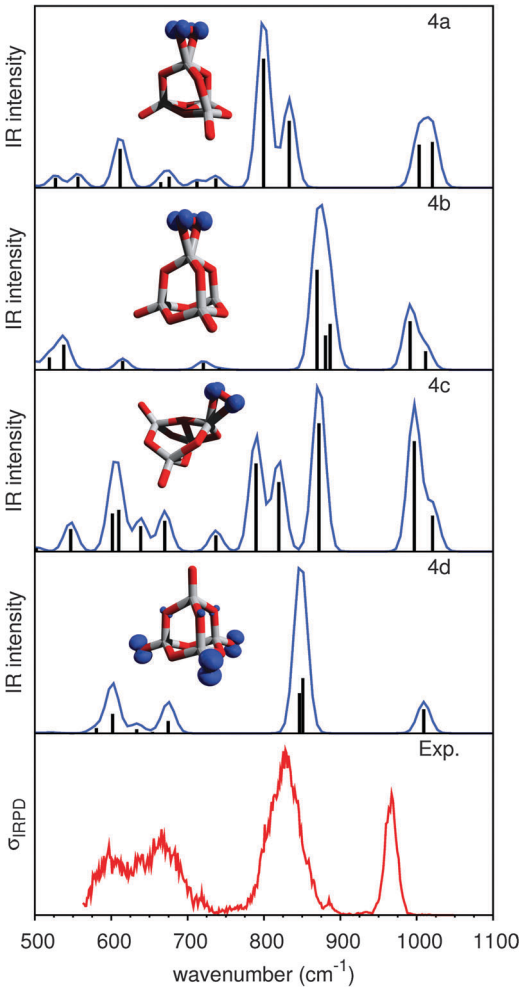


Fig. 2 Simulated IR spectra of **4a–d** and the experimental IRMPD spectrum of $Ti_4O_{10}^-$.

the spectrum (840–880 cm^{-1}) because the adamantane-like cage structure is little distorted from tetrahedral symmetry. In contrast, for **4a** and **4c** one of the bridging oxo groups is displaced towards the inside of the cage, which breaks the local symmetry and leads to modes that are spread over a larger range in the spectrum. The modes between 500 and 750 cm^{-1} mainly initiate bond stretching and bending within the cage as well as bond stretching of either Ti–O$^\bullet$ or Ti–$O_2^\bullet$ units and also strongly differ among the four candidate structures.

When comparing with the experimental spectrum, at first glance, the simulated spectrum of **4d** can qualitatively reproduce the measured IRMPD spectrum as suggested in ref. 17. However, two modes of minor intensity present at 720 and 880 cm^{-1} in the experimental spectrum are not found in the computed one. Similar modes are present in the computed spectrum of **4b** but this structure lacks vibrational modes between 550 and 750 cm^{-1} present in the experimental spectrum. The two clusters with distorted cage structures **4a** and **4c** have several modes in the 500 to 900 cm^{-1} range that are absent in the experimental spectrum. Therefore, we conclude that the experimental IRMPD spectrum is due to a mixture of **4b** and **4d** dominated by the adamantane-like cage **4d**. We note that the harmonic approximation in combination with the approximate treatment of electron correlation generally leads to overestimation of computed vibrational frequencies.[39] An experimental confirmation of the presence or absence of a terminal superoxo group would support our conclusion. Unfortunately, stretching modes of the superoxo units in **4a–c** (1202–1208 cm^{-1}) are challenging to detect experimentally because they exhibit very low intensities (3.5–5.8% compared to the most intense mode) which becomes even more difficult if the minimum structures with the superoxo unit appear with minor abundance in a mixture of cluster structures.

Our assignment raises the question why isomers that are up to 68 kJ mol^{-1} lower in energy than **4d** are apparently not (or with minor abundance) detected experimentally. One possible explanation would be that the process of cluster preparation[40] is controlled kinetically rather than thermodynamically and isomerization, condensation, and dissociation reactions are favored for **4a–c** but not for **4d**. A systematic study is beyond the scope of this article, but we can exclude the dissociation of the superoxo unit (either as O_2 or $O_2^{-\bullet}$) as a possible reaction channel because the energies of the dissociation products are of about 260 and 500 kJ mol^{-1}, respectively, higher.

C. Equilibrium structures of $(TiO_2)_3VO_{1-4}^{+/-}$

Fig. 3 shows global minimum structures for cluster compositions $(TiO_2)_3VO_{1-4}^{+/-}$ that are relevant as intermediates in the stepwise reduction of the oxygen-rich $(TiO_2)_3VO_4^-$ cluster, see Fig. 4. By removing one O^{2-} ion the latter is converted into $(TiO_2)_3VO_3^+$ in which all metal atoms are in their highest oxidation state. Among the three most stable closed-shell minimum structures, isomers **5a** and **5c** exhibit an adamantane-like cage structure with six bridging oxo groups, a terminal oxo group bonded to the vanadium atom (vanadyl group), and a terminal η^2-peroxo group bonded to one titanium atom. They merely differ by the orientation of the peroxo group, which lies either within a Ti–O–Ti plane (**5a**) or within a Ti–O–V plane (**5c**). The second most stable structure **5b** features a μ-(η^1,η^1)-peroxo unit that bridges the titanyl and vanadyl groups. Minimum structures in a triplet state are at least 15.5 kJ mol^{-1} higher in energy than the global minimum **5a**. Their structures are similar to **5a**, but they have one unpaired electron located in d-orbitals of either vanadium or titanium and another electron located in a terminal superoxo group. When comparing **5a** and **5b** we realize that the structure is energetically most favored that preserves the tetrahedral coordination of vanadium by four oxo groups and does not lead to a distortion of the cage. Therefore, peroxo and superoxo groups prefer to bond terminally to titanium. Surprisingly, a cage structure featuring two terminal oxyl radicals is 32.0 kJ mol^{-1} less stable in contrast to $(TiO_2)_3VO_4^-$.

Accepting two electrons results in reduction of the peroxo group in **5** and formation of two terminal oxo groups in the most stable $(TiO_2)_3VO_3^-$ isomers. The three minimum structures **6a–c** can be transformed into the minimum structures **4a–c** of $Ti_4O_{10}^-$, when the vanadyl group is substituted by Ti–$O_2^\bullet$. The energetic order of the clusters is preserved, however, the energy differences between the minimum structures are more pronounced for the vanadium-containing clusters.

 This journal is © the Owner Societies 2014

Published on 25 March 2014. Downloaded by Ruhr Universitat Bochum on 3/29/2023 1:12:20 PM.

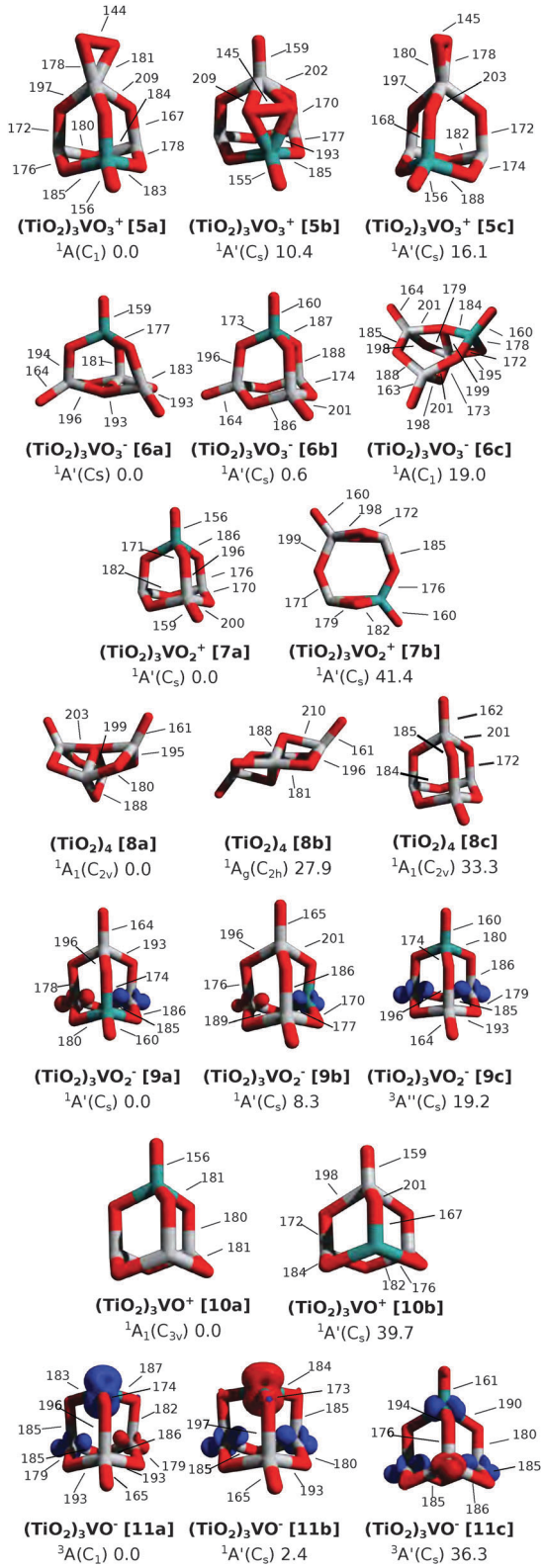


Fig. 3 Global minimum and selected local minimum structures of mono- and bimetallic titanium vanadium oxide clusters along with their electronic state and point group symmetry. Energies relative to the global minimum in kJ mol^{-1} and bond distances in pm. For open-shell systems iso-surfaces of the spin density are plotted (blue and red, iso-value 0.02).

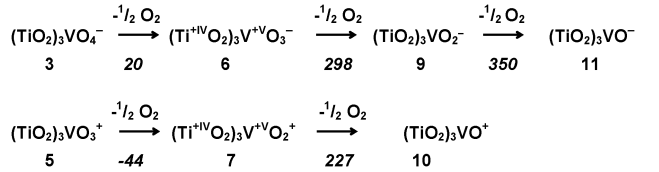


Fig. 4 Reaction energies in kJ mol^{-1}.

Removing an O^{2-} ion from $(TiO_2)_3VO_3^-$ leads to $(TiO_2)_3VO_2^+$ with the same oxidation states, +IV for Ti and +V for V. The two most stable structures **7a** and **7b** have two terminal oxo groups bonded to both vanadium and titanium. The global minimum structure features an adamantane-like cage structure and can be obtained from **6b** when one of its terminal oxo groups is eliminated. As for both $(TiO_2)V_3O_8^-$ and $(TiO_2)_2V_2O_6^-$ compositions, **1** and **2**, respectively, the compact cage structure **7a** is much more stable (41.4 kJ mol^{-1}) than the more open ring structure **7b**. The lowest energy triplet structure is 159.5 kJ mol^{-1} higher than **7a**.

Next, we discuss the most stable isomers of $(TiO_2)_4$, which is isoelectronic with $(TiO_2)_3VO_2^+$. The low-lying minimum structures of $(TiO_2)_4$ have already been investigated by several groups. Hamad *et al.* identified **8a** as the energetically most favored structure when combining global optimization techniques using interatomic potentials with refined local optimization using DFT and a double-ζ basis set including relativistic effects by effective core potentials (ECPs) for Ti (B3LYP/LANL2DZ).[41] Qu and Kroes[42] performed local optimizations using B3LYP/LANL2DZ and found that **8c** is 33 kJ mol^{-1} more stable than **8a**. In the most recent work on $(TiO_2)_4$, Li and Dixon employed a similar computational protocol (B3LYP/aug-cc-pVDZ-PP) to Hamad *et al.* and Qu and Kroes for optimizing the cluster structures.[43] Additionally, for the lowest minimum structures they used a coupled cluster with single, double, and perturbative triple excitations with a triple-ζ basis set including ECPs for Ti (CCSD(T)/aug-cc-pVTZ-PP). We obtained the three most stable structures **8a–c** in the same energetic order as they did. It is noteworthy that the structural motifs of the two most stable structures of this cluster composition, **8a–b**, are not observed when one Ti atom is replaced by V leading to the isoelectronic $(TiO_2)_3VO_2^+$ clusters **7**.

If an oxygen atom is removed from either the Ti=O or V=O bonds of **7**, one obtains for the two most stable $(TiO_2)_3VO^+$ isomers cages with a single terminal oxo group bonded to V (**10a**) or Ti (**10b**). The structure that preserves the tetrahedral bonding situation at V (**10a**) is again the most stable structure.

Compared to the fully oxidized structures **7**, the structures **10** have two additional electrons that will occupy d-states. The lowest energy structures are closed shell singlets, *i.e.* the two electrons occupy the same d-state. In structure **10a** the tetravalent vanadium stays as V^{+V}, and the two electrons occupy d-states delocalized over three Ti atoms. Structure **10b** has the two electrons delocalized over the trivalent V atom and two Ti atoms, leaving one Ti atom as Ti^{+IV}. The lowest triplet state, which is 39 kJ mol^{-1} above **10a**, has one electron on V (V^{+IV}) and one electron delocalized over the d-states of Ti.

Published on 25 March 2014. Downloaded by Ruhr Universitat Bochum on 3/29/2023 1:12:20 PM.

In the three most stable isomers of $(TiO_2)_3VO_2^-$, **9a–c**, which are partially reduced compared to the clusters **6**, two electrons are available for occupying d-orbitals of V and/or Ti. In isomers **9a** and **9c** both electrons are on Ti sites, whereas in isomer **9b** one electron is in the d-state on Ti, the other in the V-d state. For the two most stable structures **9a–b**, anti-ferromagnetic coupling of the two d-electrons with opposite spin lowers the energy substantially, by 19.2 (**9a**) and 31.5 kJ mol^{-1} (**9b**). The two spin centers on Ti–V sites are separated by two bonds and at distances of 278 pm and 265 pm in **9a** and **9b**, respectively. When ferromagnetically coupled (high-spin triplet solution) the two spin centers are further apart, 298 pm in **9c**. The proximity of the spin centers in d-states causes a strong exchange. In contrast, for the distant (600 pm) spin centers located in three oxyl radicals of **4d** exchange coupling does not play a role. Again, the most stable minimum structure **9a** has a vanadium atom tetrahedrally bonded to four oxo groups.

If another oxygen atom is removed from $(TiO_2)_3VO_2^-$, two additional electrons are available for occupying d-states in $(TiO_2)_3VO^-$, so that four electrons in total have to be distributed over the d-states on the V atom and the three Ti atoms. The three most stable structures **11a–c** represent broken-symmetry singlet and triplet solutions with unpaired electrons distributed over three (**11a** and **11b**) or four metal atoms (**11c**). In the latter case, this leads to V^{+IV} and three Ti^{+III} species. In both isomers **11a** and **11b**, there is one Ti^{+IV} left. In **11a** about two electrons are in d-states on V and on each of two Ti atoms there is about one electron, whereas in **11b** the four electrons are almost equally distributed over the V and two Ti atoms. Though cage structures with a single terminal oxo group are reasonable candidates for the global minimum structure of $(TiO_2)_3VO^-$, the electronic structure of **11a–c** with several unpaired electrons raises doubts whether a one-determinantal ansatz for the electronic structure problem is a sufficient approximation here.

D. Oxygen defect formation energies

The energy of released oxygen, with respect to half of an oxygen molecule, has been used as a descriptor for the activity of transition metal oxide catalysts in selective oxidation reactions.[11,44] It corresponds to the O defect formation energy in solid oxide catalysts. In clusters **6** and **7**, both Ti and V are in their highest oxidation states, +IV and +V, respectively. Upon oxygen removal from **6**, in the most stable isomer of $(TiO_2)_3VO_2^-$, **9a**, vanadium remains in the +V oxidation state and the two electrons left behind reduce two Ti^{+IV} to two Ti^{+III}. The structure with V^{+IV} and only one Ti^{+III}, **9b**, is 8.3 kJ mol^{-1} less stable.

The energies for reducing **6** to **9** (298 kJ mol^{-1}) and **7** to **10** (227 kJ mol^{-1}), see Fig. 4, are somewhat higher than the corresponding energies for pure vanadium oxide clusters with all V in the +V oxidation state. For $(V_2O_5)VO_3^-$ and $(V_2O_5)VO_2^+$ energies of 283 and 165 kJ mol^{-1}, respectively, have been obtained.[44] This shows that differently from CeO_2 as redox-active supporting oxide for vanadium oxide catalysts,[11] TiO_2 does not lower the energy for releasing oxygen. The calculated values for the anionic species $(TiO_2)_3VO_3^-$ (**6**) and $(V_2O_5)VO_3^-$ are also close to the value of 277 kJ mol^{-1} obtained for a model of a monomeric vanadium oxide site on the inert SiO_2 support, $OVSi_7O_{12}H_7$.[44] This points to an important difference between TiO_2 and CeO_2 as supports. Both are redox-active and accept electrons when the VO_x support system is reduced. But only for VO_x–CeO_2 this leads a significantly smaller oxygen removal (defect formation) energy. The reasons are substantial structural relaxations in the VO_x–CeO_2 system on O defect formation.[45]

IV. Conclusions

The lowest energy minimum structures of bimetallic V–Ti oxide clusters, found by application of a genetic algorithm, always featured vanadium oxo (vanadyl) groups. This fits to the conclusion from experimental studies that single vanadyl groups are present on vanadium monolayers supported on TiO_2.[7,8] These coordination of vanadium by four oxo groups constitutes a tetrahedral building unit and, hence, reduces the structural diversity for a given composition. In contrast, titanium can be coordinated by three to five oxygen atoms in terms of oxo, peroxo, or superoxo groups. Consequently, substituting an increasing number of V by Ti in the $V_{4-n}Ti_nO_{10}^-$ series destabilizes the adamantane-like cage structures in favor of more complex cluster structures, which cannot be intuitively derived from the cage motif. This also holds for oxygen-rich cluster compositions and justifies our computationally demanding GA optimization procedure. We obtained minimum structures that are, on the one hand, in line with previous investigations on Ti_4O_8[41,43] and, on the other hand, reveal isomorphisms between structures of different compositions, *e.g.* $(TiO_2)_3VO_3^-$ and $Ti_4O_{10}^-$. Moreover, we have seen that vanadium-rich or oxygen-poor cluster compositions prefer to build stable adamantane-like cages. For $Ti_4O_{10}^-$ we found three isomers that feature superoxo units and are up to 68 kJ mol^{-1} more stable than the cage with three unpaired electrons. The latter gives the best correspondence between the simulated vibrational spectrum and the experimental IRMPD spectrum, but it cannot solely explain all vibrational bands.

Upon oxygen removal from the fully oxidized $(TiO_2)_3VO_3^-$ and $(TiO_2)_3VO_2^+$ clusters one or both of the two electrons left behind occupy d-states on the Ti atoms. Nevertheless, the energies for oxygen removal are not smaller than for the pure vanadia cluster or vanadia supported on silica. This points to an important difference between TiO_2 and CeO_2 as supports. Both are redox-active and accept electrons when the VO_x support system is reduced. But only for VO_x–CeO_2 this leads to a significantly smaller oxygen removal (defect formation) energy.

Acknowledgements

This work has been supported by the German Research Foundation (DFG) within the Center of Collaborative Research "Transition metal oxide aggregates" (SFB-546).

 This journal is © the Owner Societies 2014

Published on 25 March 2014. Downloaded by Ruhr Universitat Bochum on 3/29/2023 1:12:20 PM.

References

1 B. M. Weckhuysen and D. E. Keller, *Catal. Today*, 2003, **78**, 25.
2 I. E. Wachs, *Catal. Today*, 2005, **100**, 79.
3 P. Forzatti, *Appl. Catal., A*, 2001, **222**, 221.
4 M. A. Ba~nares, *Catal. Today*, 1999, **51**, 319.
5 A. Khodakov, B. Olthof, A. T. Bell and E. Iglesia, *J. Catal.*, 1999, **181**, 205.
6 B. Beck, M. Harth, N. G. Hamilton, C. Carrero, J. J. Uhlrich, A. Trunschke, S. Shaikhutdinov, H. Schubert, H.-J. Freund, R. Schlögl, J. Sauer and R. Schomäcker, *J. Catal.*, 2012, **296**, 120.
7 G. C. Bond and K. Bruckman, *Faraday Discuss.*, 1981, **72**, 235.
8 E. Wachs, R. Y. Saleh, S. S. Chan and C. C. Chersich, *Appl. Catal.*, 1985, **15**, 339.
9 N. Magg, B. Immaraporn, J. B. Giorgi, T. Schroeder, M. Bäumer, J. Döbler, Z. Wu, E. Kondratenko, M. Cherian, M. Baerns, P. C. Stair, J. Sauer and H.-J. Freund, *J. Catal.*, 2004, **226**, 88.
10 M. Baron, H. Abbott, O. Bondarchuk, D. Stacchiola, A. Uhl, S. Shaikhutdinov, H.-J. Freund, C. Popa, M. Ganduglia-Pirovano and J. Sauer, *Angew. Chem., Int. Ed.*, 2009, **48**, 8006.
11 M. V. Ganduglia-Pirovano, C. Popa, J. Sauer, H. Abbott, A. Uhl, M. Baron, D. Stacchiola, O. Bondarchuk, S. Shaikhutdinov and H.-J. Freund, *J. Am. Chem. Soc.*, 2010, **132**, 2345.
12 L. Jiang, T. Wende, P. Claes, S. Bhattacharyya, M. Sierka, G. Meijer, P. Lievens, J. Sauer and K. R. Asmis, *J. Phys. Chem. A*, 2011, **115**, 11187.
13 K. Böhme and H. Schwarz, *Angew. Chem., Int. Ed.*, 2005, **44**, 2336.
14 K. A. Zemski, D. R. Justes and A. W. Castleman, *J. Phys. Chem. B*, 2002, **106**, 6136.
15 J. E. Mann, D. W. Rothgeb, S. E. Waller and C. C. Jarrold, *J. Phys. Chem. A*, 2010, **114**, 11312.
16 Z.-C. Wang, X.-N. Wu, Y.-X. Zhao, J.-B. Ma, X.-L. Ding and S.-G. He, *Chem. – Eur. J.*, 2011, **17**, 3449.
17 E. Janssens, G. Santambrogio, M. Brümmer, L. Wöste, P. Lievens, J. Sauer, G. Meijer and K. R. Asmis, *Phys. Rev. Lett.*, 2006, **96**, 233401.
18 K. R. Asmis, G. Santambrogio, M. Brümmer and J. Sauer, *Angew. Chem.*, 2005, **117**, 3182; K. R. Asmis, G. Santambrogio, M. Brümmer and J. Sauer, *Angew. Chem., Int. Ed.*, 2005, **44**, 3122.
19 A. D. Becke, *Phys. Rev. A: At., Mol., Opt. Phys.*, 1988, **38**, 3098.
20 C. Lee, W. Yang and R. G. Parr, *Phys. Rev. B: Condens. Matter Mater. Phys.*, 1988, **37**, 785.
21 A. D. Becke, *J. Chem. Phys.*, 1993, **98**, 5648.
22 A. Schäfer, C. Huber and R. Ahlrichs, *J. Chem. Phys.*, 1994, **100**, 5829.
23 E. Janssens, S. M. Lang, M. Brummer, A. Niedziela, G. Santambrogio, K. R. Asmis and J. Sauer, *Phys. Chem. Chem. Phys.*, 2012, **14**, 14344.
24 M. Sierka, *Prog. Surf. Sci.*, 2010, **85**, 398.
25 M. Sierka, J. Döbler, J. Sauer, G. Santambrogio, M. Brümmer, L. Wöste, E. Janssens, G. Meijer and K. R. Asmis, *Angew. Chem., Int. Ed.*, 2007, **46**, 3372.
26 G. Santambrogio, M. Brümmer, L. Wöste, J. Döbler, M. Sierka, J. Sauer, G. Meijer and K. R. Asmis, *Phys. Chem. Chem. Phys.*, 2008, **10**, 3992.
27 G. Santambrogio, E. Janssens, S. Li, T. Siebert, G. Meijer, K. R. Asmis, J. Döbler, M. Sierka and J. Sauer, *J. Am. Chem. Soc.*, 2008, **130**, 15143.
28 A. M. Burow, T. Wende, M. Sierka, R. W lodarczyk, J. Sauer, P. Claes, L. Jiang, G. Meijer, P. Lievens and K. R. Asmis, *Phys. Chem. Chem. Phys.*, 2011, **13**, 19393.
29 R. Ahlrichs, M. Bär, M. Häser, H. Horn and C. Kölmel, *Chem. Phys. Lett.*, 1989, **162**, 165.
30 TURBOMOLE V6.2 2010, a development of University of Karlsruhe and Forschungszentrum Karlsruhe GmbH, 1989–2007, TURBOMOLE GmbH, since 2007, available from http://www.turbomole.com.
31 F. Weigend and R. Ahlrichs, *Phys. Chem. Chem. Phys.*, 2005, **7**, 3297.
32 M. Sierka, A. Hogekamp and R. Ahlrichs, *J. Chem. Phys.*, 2003, **118**, 9136.
33 M. Sierka, B. Helmich and R. Włodarczyk, 2013, Program DoDo, Humboldt-Universität zu Berlin, since 2012 Friedrich-Schiller-Universität Jena.
34 R. Bauernschmitt and R. Ahlrichs, *J. Chem. Phys.*, 1996, **104**, 9047.
35 F. Weigend, M. Häser, H. Patzelt and R. Ahlrichs, *Chem. Phys. Lett.*, 1998, **294**, 143.
36 P. Deglmann, F. Furche and R. Ahlrichs, *Chem. Phys. Lett.*, 2002, **362**, 511.
37 S. F. Vyboishchikov and J. Sauer, *J. Phys. Chem. A*, 2001, **105**, 8588.
38 D. A. Dougherty, *Acc. Chem. Res.*, 1991, **24**, 88.
39 J. A. Pople, H. B. Schlegel, R. Krishnan, D. J. Defrees, J. S. Binkley, M. J. Frisch, R. A. Whiteside, R. F. Hout and W. J. Hehre, *Int. J. Quantum Chem.*, 1981, **20**, 269.
40 W. Bouwen, P. Thoen, F. Vanhoutte, S. Bouckaert, F. Despa, H. Weidele, R. E. Silverans and P. Lievens, *Rev. Sci. Instrum.*, 2000, **71**, 54.
41 S. Hamad, C. R. A. Catlow, S. M. Woodley, S. Lago and J. A. Mejías, *J. Phys. Chem. B*, 2005, **109**, 15741.
42 Z.-w. Qu and G.-J. Kroes, *J. Phys. Chem. B*, 2006, **110**, 8998.
43 S. Li and D. A. Dixon, *J. Phys. Chem. A*, 2008, **112**, 6646.
44 J. Sauer and J. Döbler, *Dalton Trans.*, 2004, 3116.
45 C. Penschke, J. Paier and J. Sauer, *J. Phys. Chem. C*, 2013, **117**, 5274.